2D Hydrodynamics of an incompressible fluid with viscosity in steady state

Mark Danovich

August 11, 2012

Abstract

We solve numerically the flow of an incompressible fluid in 2D with viscosity past a rectangular obstacle in steady state. We solve the hydrodynamical equations for the stream and vorticity functions using Gauss-Seidel relaxation method and study the behaviour of the solution for different Reynolds numbers and grid spacings.

1 Introduction

The fluid equations in steady-state ($\frac{\partial}{\partial t}=0$) are the continuity and Navier-Stokes equations:

$$\nabla\cdot\vec{v}=0$$

$$(\vec{v}\cdot\nabla)\vec{v}=-\frac{1}{\rho}\nabla p+\nu\nabla^2\vec{v}$$

Where $\vec{v}$ is the fluid velocity field, ρ is the density field, P is the pressure field and ν is the kinematical viscosity. We assume here that the changes in density with position are negligible due to uniform fluid temperature.

Writing these equations in Cartesian coordinates and defining the velocity field components, $u=\vec{v}_x, v=\vec{v}_y$:

$$\frac{\partial u}{\partial x}+\frac{\partial v}{\partial y}=0 \tag{1}$$

$$u\frac{\partial u}{\partial x}+v\frac{\partial u}{\partial y}=-\frac{1}{\rho}\frac{\partial P}{\partial x}+\nu(\frac{\partial^2 u}{\partial x^2}+\frac{\partial^2 u}{\partial y^2}) \tag{2}$$

$$u\frac{\partial v}{\partial x}+v\frac{\partial v}{\partial y}=-\frac{1}{\rho}\frac{\partial P}{\partial y}+\nu(\frac{\partial^2 v}{\partial x^2}+\frac{\partial^2 v}{\partial y^2}) \tag{3}$$

For our purpose it will be convenient to solve instead for the stream function $\psi(x,y)$ and vorticity function $\xi(x,y)$, which are defined by $u=\frac{\partial\psi}{\partial y}, v=-\frac{\partial\psi}{\partial x}$ (it can be shown that it is always possible to find such a function for a fluid flow field) and $\xi=\frac{\partial u}{\partial y}-\frac{\partial v}{\partial x}$. The importance of the stream function is that constant lines of ψ are tangent to the velocity vector field and thus these lines represent the stream lines of the fluid elements (this is easily seen from $(\vec{v}\cdot\nabla)\psi=0$). We would like to transform the fluid equations (1)-(3) to equations for ψ,ξ and P.

Using the definition of the stream and vorticity functions we get the first equation:

$$\nabla^2 \psi = \xi \tag{4}$$

The second equation we get by differentiating equation (2) by y and subtracting from it equation (3) differentiated by x.

$$\nu \nabla^2 \xi = \frac{\partial \psi}{\partial y}\frac{\partial \xi}{\partial x} - \frac{\partial \psi}{\partial x}\frac{\partial \xi}{\partial y} \tag{5}$$

We see that P doesn't appear in these equations. In a similar way by differentiating equation (2) by x and adding equation (3) differentiated by y we get an equation for P.

$$\nabla^2 P = 2\rho(\frac{\partial^2 \psi}{\partial x^2}\frac{\partial^2 \psi}{\partial y^2} - (\frac{\partial^2 \psi}{\partial x \partial y})^2) \tag{6}$$

Our problem consists of solving the non-linear elliptic coupled PDEs (4) and (5) for the flow in 2D of a fluid flowing at a constant velocity v_0 towards a rectangular obstacle of given dimensions as shown in Fig. 1.

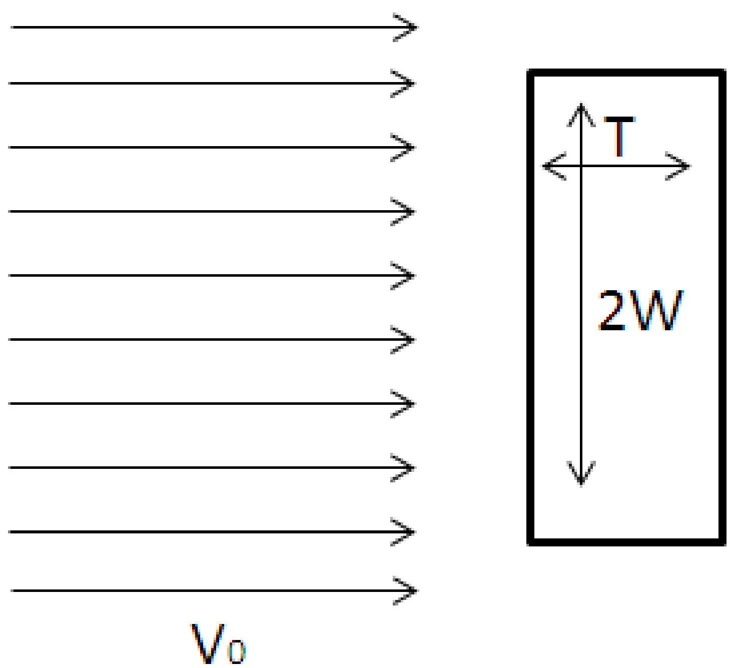

Figure 1: Schematic description of the general problem.

2 The Method

We solve equations (4),(5) on a 2D Cartesian grid with spacing h and $nx \times ny$ grid points. The region of solution and the obstacle dimensions are shown in Fig. 2. Since the flow has reflection symmetry through $y = 0$ it is sufficient and more economical to solve only the upper half of the flow (we can then in principal reflect the solution through $y = 0$ and get the full flow). We label the boundaries of the flow region by A-H where we specify appropriate boundary conditions.

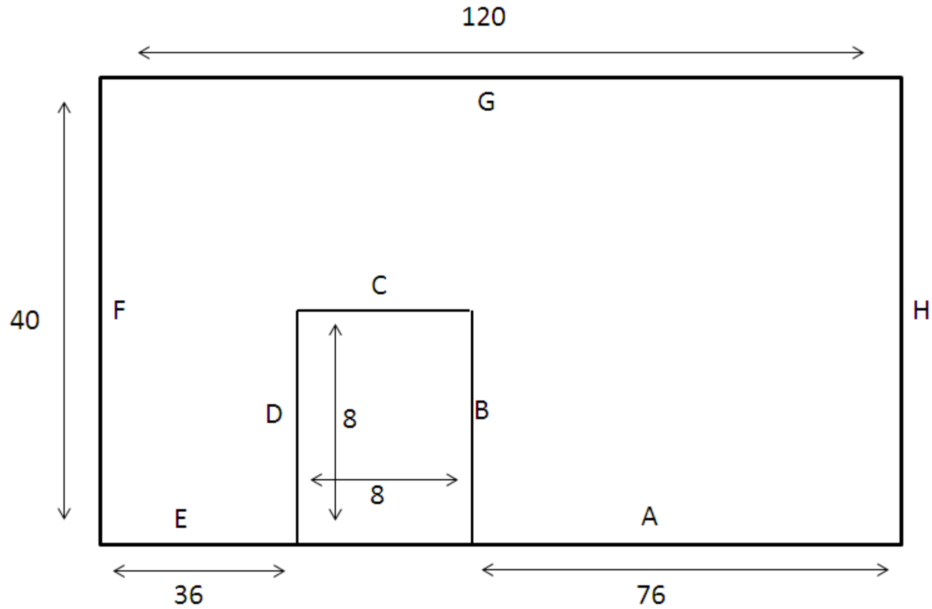

Figure 2: The region we wish to solve with the labelled boundaries and specified size for the boundaries and obstacle.

b.c. for ψ :
A-E: $\psi = 0$ (symmetry about y=0 and velocity perpendicular to obstacle is 0 therefore all this boundary is a line of constant ψ and we can arbitrarily choose $\psi = 0$).
F: $\frac{\partial \psi}{\partial x} = 0$ (undisturbed incoming flow).
G: $\frac{\partial \psi}{\partial y} = v_0$ (undisturbed flow high above the obstacle).
H: $\frac{\partial \psi}{\partial x} = 0$ (far enough from the obstacle we demand no changes in ψ).
b.c. for ξ :
A,E: $\xi = 0$ (symmetry about y=0).
F: $\xi = 0$ (undisturbed incoming flow).
G: $\xi = 0$ (undisturbed flow high above the obstacle).
H: $\frac{\partial \xi}{\partial x} = 0$ (far enough from the obstacle we demand no changes in ξ).
B,C,D: $\xi = \frac{\partial^2 \psi}{\partial y^2}$ (Taylor expanding ψ near the obstacle and using $\frac{\partial \psi}{\partial y} = 0$, $\frac{\partial v}{\partial x} = 0$ on the obstacle, tangential and perpendicular velocities are zero).

For convenience we will work with dimensionless quantities by writing ψ in units of $v_0 h$ and ξ in units of v_0/h.

First, we transform the PDEs to difference equations on the grid, divide both sides by $v_0 h$ and rearrange the factors of h and v_0 to get equations (4) and (5) in terms of the new ψ and ξ:

$$\delta_i^2 \psi_{i,j} + \delta_j^2 \psi_{i,j} = \xi_{i,j}$$

$$\delta_i^2 \xi_{i,j} + \delta_j^2 \xi_{i,j} = \frac{R}{4}[\delta_j \psi_{i,j} \delta_i \xi_{i,j} - \delta_i \psi_{i,j} \delta_j \xi_{i,j}]$$

With the operators defined by: $\delta_i^2 \psi_{i,j} = \psi_{i+1,j} - 2\psi_{i,j} + \psi_{i-1,j}$, $\delta_i \psi_{i,j} = \psi_{i+1,j} - \psi_{i-1,j}$, and similar definitions for j. The grid Reynolds number is defined by: $R = \frac{v_0 h}{\nu}$. We remind that the physical Reynolds number is defined for an obstacle with cross section $2W$ by: $R_e = \frac{2Wv_0}{\nu}$, therefore the two Reynolds numbers are related by: $R_e = \frac{2W}{h}R$.

Expanding these difference equations and rearranging we get the final equations for ψ and ξ at the grid point (i, j), which we will solve iteratively using the Gauss-Seidel relaxation method.

$$\psi_{i,j} = \frac{1}{4}(\psi_{i+1,j} + \psi_{i-1,j} + \psi_{i,j+1} + \psi_{i,j-1} - \xi_{i,j}) \tag{7}$$

$$\xi_{i,j} = \frac{1}{4}(\xi_{i+1,j}+\xi_{i-1,j}+\xi_{i,j+1}+\xi_{i,j-1}) - \frac{R}{16}[(\psi_{i,j+1}-\psi_{i,j-1})(\xi_{i+1,j}-\xi_{i-1,j})-(\psi_{i+1,j}-\psi_{i-1,j})(\xi_{i,j+1}-\xi_{i,j-1})] \tag{8}$$

Next, we write the boundary conditions using the dimensionless ψ, ξ and using grid indices.

b.c. for ψ :
A-E: $\psi_{i,j} = 0$
F: $\psi_{1,j} = \psi_{2,j}$
G: $\psi_{i,ny} = \psi_{i,ny-1} + 1$
H: $\psi_{nx,j} = \psi_{nx-1,j}$
b.c. for ξ :
A,E,F,G: $\xi_{i,j} = 0$
H: $\xi_{nx,j} = \xi_{nx-1,j}$
B,C,D: $\xi_{i,j} = 2\psi_{i+1,j}$, $\xi_{i,j} = 2\psi_{i,j+1}$, $\xi_{i,j} = 2\psi_{i-1,j}$

In the corners between B-C and D-C we will use the average between the two possible values, B-C: $\xi_{i,j} = \psi_{i+1,j} + \psi_{i,j+1}$, D-C: $\xi_{i,j} = \psi_{i-1,j} + \psi_{i,j+1}$.

We note that near the boundaries with b.c. of the Neumann type and in the corners, equations (7) and (8) for $\psi_{i,j}$ and $\xi_{i,j}$ are modified. By substituting the above Neumann type b.c. and rearranging we get for the grid cells near the boundaries and corners the following difference equations:

F($i = 2, j = 2 \to ny - 1$):
$\psi_{i,j} = \frac{1}{3}(\psi_{i+1,j} + \psi_{i,j+1} + \psi_{i,j-1} - \xi_{i,j})$
G($i = 2 \to nx - 1, j = ny - 1$):
$\psi_{i,j} = \frac{1}{3}(\psi_{i+1,j} + \psi_{i-1,j} + \psi_{i,j-1} + 1 - \xi_{i,j})$
H($i = nx - 1, j = 2 \to ny - 1$):
$\psi_{i,j} = \frac{1}{3}(\psi_{i-1,j} + \psi_{i,j+1} + \psi_{i,j-1} - \xi_{i,j})$
$\xi_{i,j} = [\xi_{i,j+1}+\xi_{i,j-1}+\xi_{i-1,j}+\frac{R}{4}(\xi_{i-1,j}(\psi_{i,j+1}-\psi_{i,j-1})+(\psi_{i+1,j}-\psi_{i-1,j})(\xi_{i,j+1}-\xi_{i,j-1}))]/(3+\frac{R}{4}(\psi_{i,j+1} - \psi_{i,j-1}))$

Inner Corners:
F-G($i = 2, j = ny - 1$):
$\psi_{i,j} = \frac{1}{2}(\psi_{i+1,j} + \psi_{i,j-1} + 1 - \xi_{i,j})$
H-G($i = nx - 1, j = ny - 1$):
$\psi_{i,j} = \frac{1}{2}(\psi_{i-1,j} + \psi_{i,j-1} + 1 - \xi_{i,j})$

The boundry conditions at the outer corners between F-G and H-G are calculated by averaging the two Neumann b.c. specified there.

The solution of equations (7),(8) with the given boundary conditions is done iteratively using the Gauss-Seidel method where a relaxation parameter $w = 0.1$ or 0.3 is used for relaxing the ψ and ξ grids restricted to the above given boundary conditions. We first make an initial guess either the free flow solution ($\psi_{i,j} = (j-1)h$, $\xi_{i,j} = 0$) or use a previous solution with a lower R, then we make one iteration relaxing ψ then use the new ψ to set the Dirichlet b.c. on the obstacle for ξ and make one iteration relaxing ξ, we repeat this process until the difference between two iterations is smaller than a defined value $\epsilon = 10^{-7}$.

3 Results

3.1 Laminar and Turbulent flows

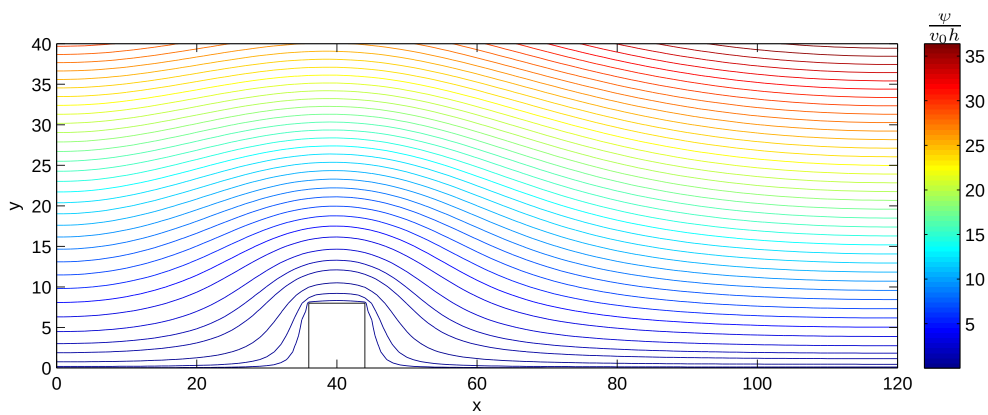

Figure 3: Stream function ψ contour plot, for $h = 1$ and $R = 0.01$.

In Fig. 3 we see the lines of constant ψ, which are the stream lines of the flow for $h = 1, R = 0.01$, the physical Reynolds number is $R_e = 0.16$. The flow is deep in the laminar regime, it passes the obstacle smoothly and symmetrically, and there are no vortices near the obstacle as expected.

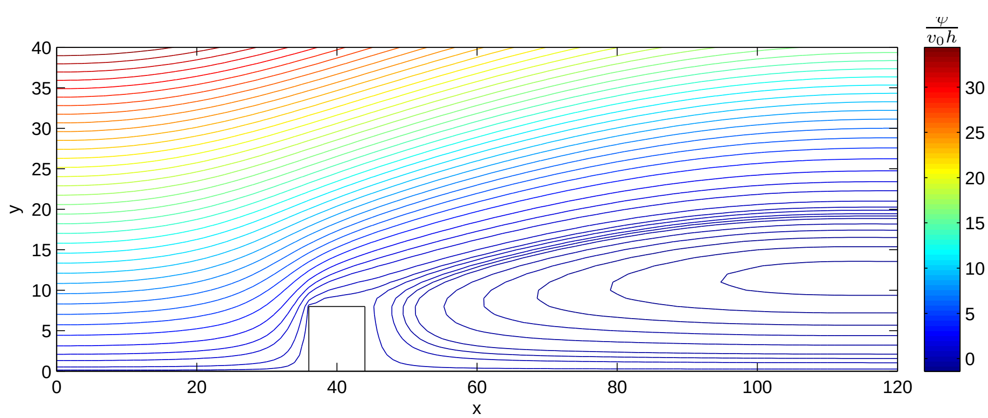

Figure 4: Stream function ψ contour plot, for $h = 1$ and $R = 4$.

In Fig. 4 we see the lines of constant ψ, which are the stream lines of the flow for $h = 1, R = 4$, the physical Reynolds number is $R_e = 64$. The flow is highly turbulent, we see large vortices following the far side of the obstacle, the regular flow separated from the obstacle and in the large area left below there are large vortices which continue beyond our region. The vortices contain fluid flowing in the opposite direction to the original flow, and these opposite flow is what triggered their formation.

3.2 Critical R_e

The determination of the critical R_e separating the laminar and turbulent flows regimes depends on how we define them. A possible way is to find when there begins to be a flow close to the far side of obstacle in the positive y direction, opposite to the regular flow in the laminar regime. Using the definition $v = -\frac{\partial\psi}{\partial x}$, we calculate the difference equation $-\frac{\psi_{i+1,j}-\psi_{i,j}}{h}$ near the far side of the obstacle, when this value is positive there is a flow in the positive y direction opposite to the regular flow coming from the top of the obstacle and this leads to the creation of vortices.

3.2.1 $h = 1$

We find that at $R_e = 2.4(R = 0.15)$, there begins to be an opposite flow in the lower half of the obstacle with velocities of the order of 10^{-4} relative to $v_0 = 1$, this is very small and implies the very early turbulent regime of the flow.

In Fig. 5 we see the approximate start of the turbulent flow regime at the top figure with $R = 0.15, R_e = 2.4$. We see in the contour plot a small closed loop which implies a small vortex with opposite flow. We further show using higher Reynolds numbers, the development of the vortices. We see the regular, laminar flow separating from the far end of the obstacle as the flow becomes more turbulent. Also, we see more vortices of different sizes and contour levels are forming one inside the other, filling the gap formed between the far end of the obstacle and the separated laminar flow above the obstacle, these vortices indicate flows in the opposite direction of the regular flow.

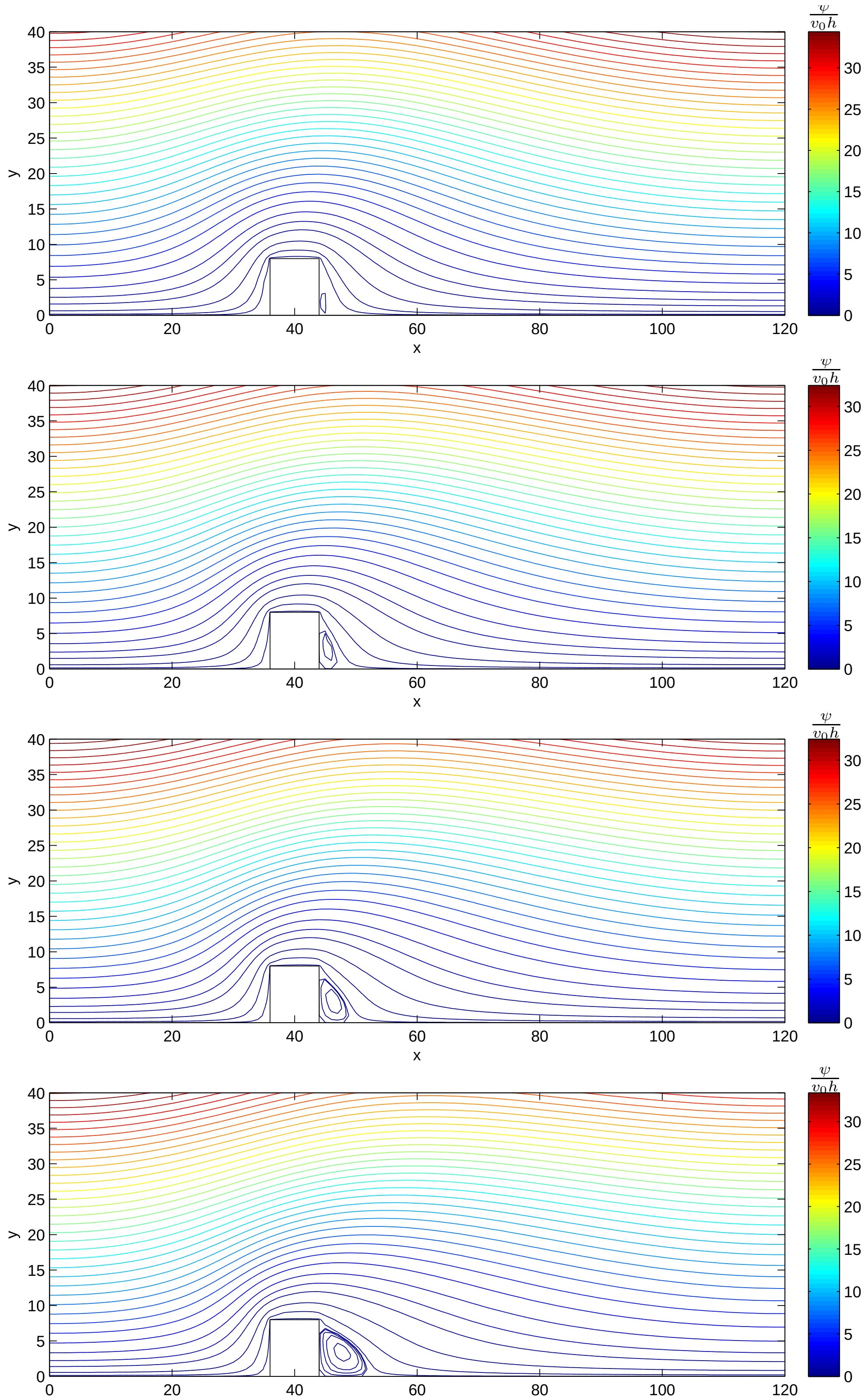

Figure 5: Stream function ψ contour plots, for $h = 1$ and (top to bottom): $R = 0.15, 0.25, 0.35, 0.5$, ($R_e = 2.4, 4, 5.6, 8$).

3.2.2 $h = 0.5$

We can anticipate from the relation $R_e = \frac{2W}{h} R$ that for $h = 0.5$, since for the same R we get R_e twice as big, we should enter the turbulent flow regime at a lower R but at approximately the same R_e since this is the physical parameter of the real problem. Similarly to the analysis for $h = 1$ we find opposite flow near the far end of the obstacle at approximately $R = 0.07, R_e = 2.24$. We show in addition the flow pattern at a higher R showing the development of the vortex in the more turbulent regime.

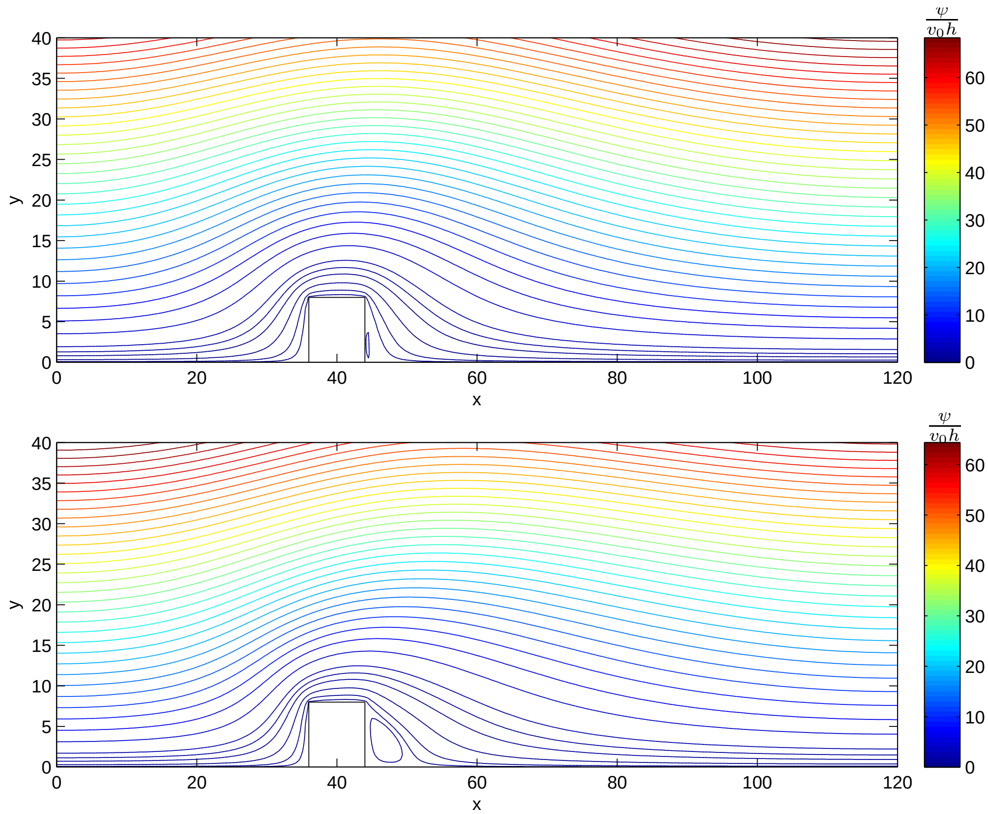

Figure 6: Stream function ψ contour plots, for $h = 0.5$ and $R = 0.07, R_e = 2.24$ (top), $R = 0.2, R_e = 6.4$ (bottom).

4 $h = 1$ and $h = 0.5$ grid spacing comparison

We compare the solutions for the same physical R_e but different grid spacings h. We use $R_e = 16$ which is above the critical Reynolds number.

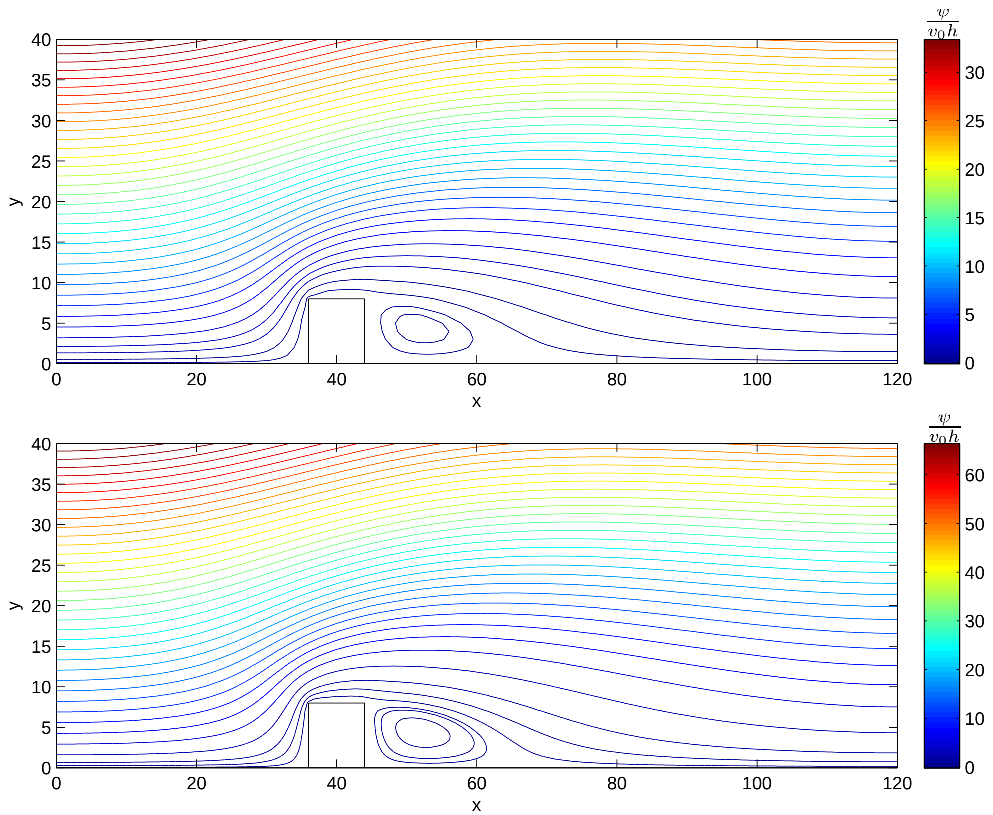

Figure 7: Stream function ψ contour plots, for $h = 1, R = 1, R_e = 16$ (top) and $h = 0.5, R = 0.5, R_e = 16$ (bottom).

In Fig. 7 we see the two solutions for ψ with the specified parameters (same R_e) and with similar contour levels. Far from the obstacle we don't see any significant differences between the two plots. Near the obstacle we see some difference in the spacing of the contours and the number of vortices after the obstacle. This is probably due to the better resolution of the $h = 0.5$ solution allowing to better resolve these more complex details of the flow. Another expected difference can be seen by looking at the stream line closest to the near corner of the obstacle, there we see that in the $h = 1$ grid it is a little less smooth with more sharp edges than the similar stream line in the $h = 0.5$ grid, which is more smooth and better resolved.

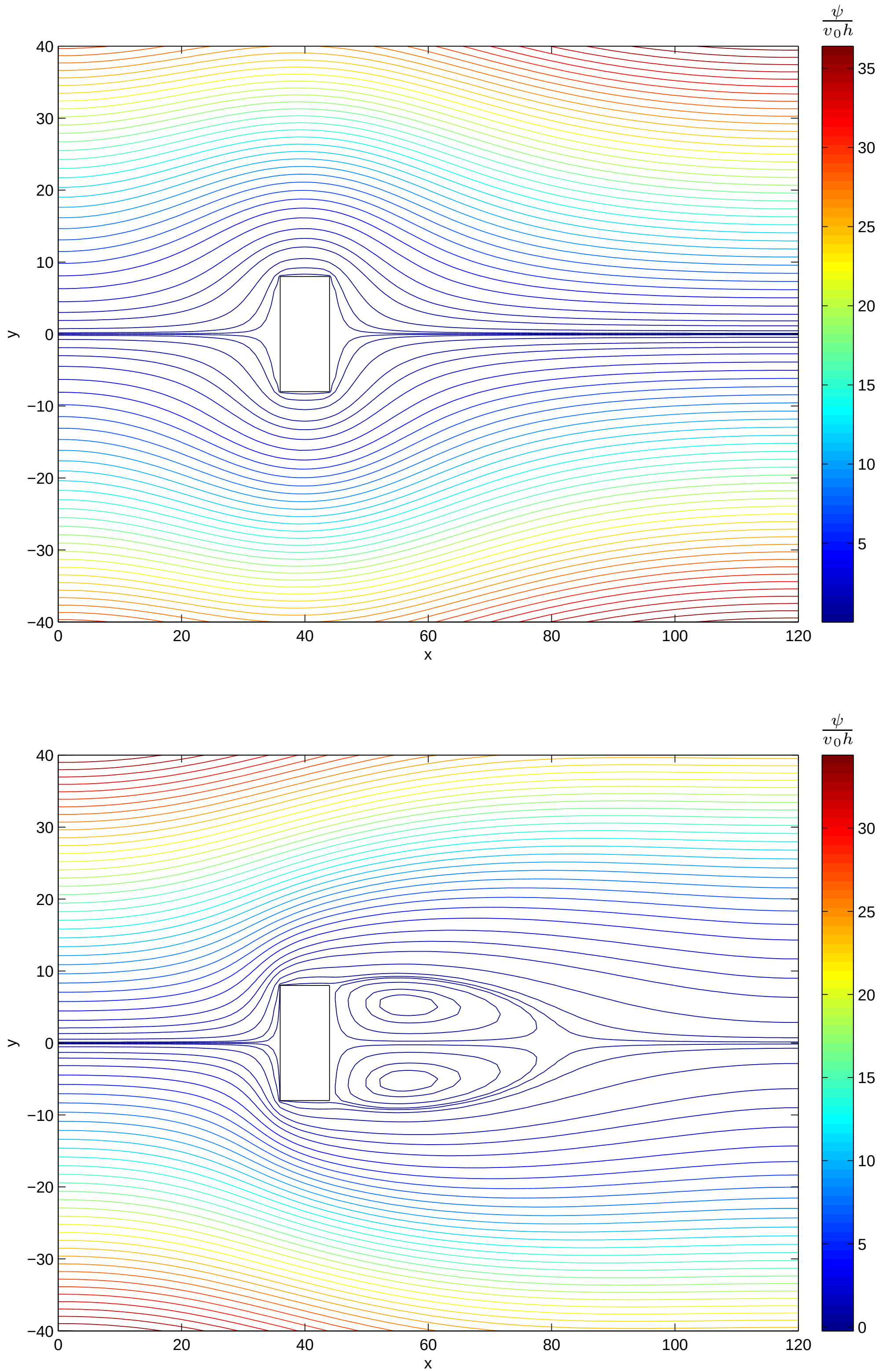

Figure 8: Stream function ψ contour plots showing the full symmetrical flow about $y = 0$ (obtained by simply reflecting the upper half solution), for $h = 1, R = 0.01, R_e = 0.16$ (top) and $h = 1, R = 1.5, R_e = 24$ (bottom).